

Andrzej ZABORSKI*

ANALYSIS OF THE WEAR PROCESS OF SURFACE LAYERS AFTER BURNISHING

ANALIZA PRZEBIEGU PROCESU ZUŻYWANIA WARSTW WIERZCHNICH PO NAGNIATANIU

Key words:

burnishing treatment, surface layer, surface wear.

Abstract:

The paper presents the results of an analysis of the wear process under conditions of dry technical friction of surface layers after selecting external surface pressure burnishing methods. The possibility of making changes in the burnishing process leading to an increase in resistance to wear under conditions of a simulated exploitation process is described. The possibility of conscious control of the process of material deformation in the zone of contact between the tool and the workpiece in the course of the surface layer formation process by changing the method and technological parameters of the pressure burnishing process is used. The course and results of the wear process of surfaces pressure burnished with a rolling ball, disc, and sliding ball are analysed. A description of the wear mechanism and comparative results of the wear of the surfaces tested are presented.

Słowa kluczowe:

obróbka nagniataniem, warstwa wierzchnia, zużycie powierzchni.

Streszczenie:

W opracowaniu przedstawiono wyniki analizy przebiegu procesu zużycia w warunkach tarcia technicznego suchego warstw wierzchnich po wybranych sposobach obróbki nagniataniem naporowym powierzchni zewnętrznych. Opisano możliwość dokonania zmian w procesie nagniatania prowadzących do wzrostu odporności na zużycie w warunkach symulowanego procesu eksploatacji. Wykorzystano do tego możliwość świadomego sterowania przebiegiem procesu odkształcania materiału w strefie kontaktu narzędzia z przedmiotem obrabianym w trakcie procesu konstituowania warstwy wierzchniej na drodze zmiany sposobu i parametrów technologicznych procesu nagniatania naporowego. Przeanalizowano przebieg i rezultaty procesu zużycia powierzchni nagniatanych naporowo tocznie kulką i krążkiem oraz powierzchni nagniatanej ślizgowo kulką. Przedstawiono opis mechanizmu zużycia i wyniki porównawcze wartości zużycia badanych powierzchni.

INTRODUCTION

Burnishing treatment is one of the most widespread surface engineering methods allowing conscious control of the functional properties of the forming surface layers [L. 1–6]. It allows a relatively easy and inexpensive improvement of complex surface layer characteristics that are important from a user's point of view [L. 7–13]. Burnishing changes the metal's mechanical and physical properties [L. 14–18]. The surface treatment by burnishing

makes it possible to improve the resistance of the obtained surface layers to mechanical, thermal and chemical factors occurring during exploitation [L. 19–22]. This resistance is achieved by creating a new, more favourable structure with a significantly higher hardness and modifying residual stresses' state and distribution [L. 6, 14, 23]. This is due to changes occurring in the surface layer during burnishing as a result of processes taking place within the deformation zone [L. 5, 6, 24]. The studies on the wear processes of burnished surface

* ORCID: 0000-0003-1738-5034. Czestochowa University of Technology, Department of Technology and Automation, Czestochowa, Poland, email: andrzej.zaborski@pcz.pl.

layers, carried out by the author for several years, unambiguously confirm that the characteristics of the surface layers obtained are largely determined by way of burnishing treatment and the deformation scheme applied to determine the occurrence of a specific technological state of the surface layer [L. 24. 25].

EXPERIMENTAL TESTING OF THE WEAR PROCESS

Preparation of experimental testing of the wear process

In the conducted testing of wear under frictional conditions, the test bench made for the conducted wear testing was used (Fig. 1). The bench was constructed using a universal lathe type CU-500 equipped with a hydraulic device for forcing the pressure of a cast iron counter-specimen against a steel specimen. It allowed continuous measurement of the friction force and, indirectly, of the coefficient of friction and the measurement

of linear wear (on the diameter) using an induction sensor mounted on a moving slide pushed against the specimen for the duration of the measurements. The wear of sliding pairs was measured in the tests, with a specimen made of C55 steel acting as a pivot and the counter-specimen made of EN-GJL-250 cast iron as a pan (Fig. 1d and e). The wear process was carried out under conditions of technically dry friction. The pressure (p) relative velocity (v) of the counter specimen to the test surface was determined from the permissible value for a given friction pair (steel – cast iron) of $p v_{\text{dop}} = 1.6 \text{ MPa} \cdot \text{m/s}$ and the recommended relative pressure of $2 \div 2.5 \text{ MPa}$. Assumed rotational speed $n = 315 \text{ rpm}$ ($v = 39.58 \text{ m/min}$) and relative pressure $p = 2.43 \text{ MPa}$. The results of the wear measurement were read out at six points on the circumference of the specimen using an inductive sensor with a digital reading device. The value was read continuously using the inductive sensor. Knowing the friction force (T) and the contact force (N) of the counter-specimen to the test surface allowed the average coefficient of friction μ to be determined as a function of the contact time.

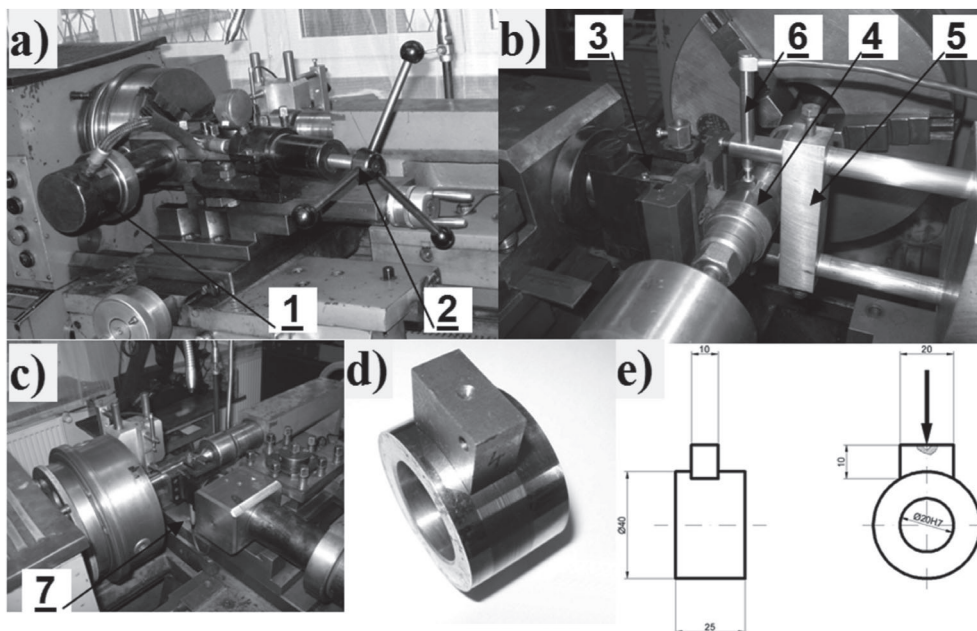


Fig. 1. Test bench for measurement and analysis of the wear process (a), wear measurement (b), view of the cylinder head (c), the tested sliding pair (d), load scheme and dimensions of the specimens (e): 1 – hydraulic cylinder, 2 – pressure regulator, 3 – head with the counter-specimen, 4 – friction specimen, 5 – measuring sliding, 6 – inductive sensor for wear measurement, 7 – inductive sensor for the recording of friction force

Rys. 1. Stanowisko do pomiaru i analizy przebiegu procesu zużycia (a), pomiar zużycia (b), widok głowicy z siłownikiem (c), badana para ślizgowa (d), schemat obciążenia i wymiary próbek (e): 1 – siłownik hydrauliczny, 2 – regulator ciśnienia, 3 – głowica z przeciwpróbką, 4 – próbka ścierana, 5 – sianie pomiarowe, 6 – czujnik indukcyjny do pomiaru zużycia, 7 – czujnik indukcyjny do rejestracji siły tarcia

The value of linear wear was determined by the diameter of the tested surfaces (fig.1b). However, the accuracy of measurement carried out in this manner was often not satisfactory, which resulted both from different wear values at different points of the tested surfaces and from changes in the temperature of the tested surfaces occurring during the wear process, which undoubtedly had an impact on reducing the accuracy of the wear

measurement itself. This necessitated the search for other methods that would precisely determine the exact value of the wear obtained. One of the options used in practice during the study was determining the course of the roughness profile in the transition area between the surface not involved in friction and the surface after friction. The obtained profile allowed for very precise determination of linear wear in any area of the analysed surface (**Fig. 2**).

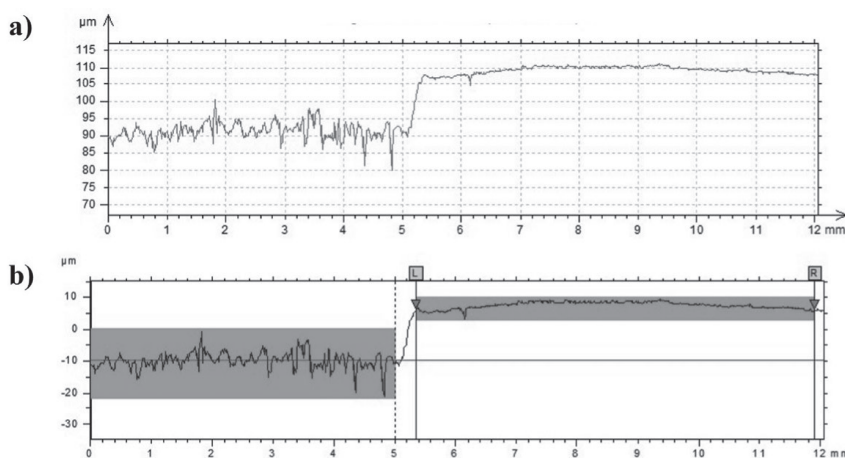


Fig. 2. Wear zone after rolling pressure burnishing: a – distinguished profile of the transition zone between the worn out and the non-worn area, b – determination of the fault height

Rys. 2. Strefa zużycia po obróbce tocznym nagniataniem naporowym: a wyodrębniony profil strefy przejścia pomiędzy obszarem zużytym i obszarem nie poddanym zużyciu, b – wyznaczenie wysokości uskoku

Three surface groups were analysed: rolling ball pressure burnishing, rolling disc pressure burnishing and sliding ball burnishing. In order to homogenise the structure, the C55 steel bars were hardened (austenitising – 840°C, water cooling) and highly tempered (500°C, 2.5h) before the specimens were made. They were then made into sleeve-shaped specimens. After machining, the specimens were subjected to hardness measurements. The average hardness was 25.05 ± 0.73 HRC. The finishing parameters prior to burnishing were: $n = 800$ rpm, $v = 100.5$ m/min, $f = 0.102$ mm/rev. The burnished C55 steel specimens acted as a pivot and the EN-GJL-250 cast iron counter-specimens as a pan during wear. The counter-specimens were made of a single piece of EN-GJL-250 cast iron. They were cubes of $10 \times 15 \times 20$ mm, with an undercut in the shape of a radius equal to that of the test specimen (i.e., 20 mm). The average hardness was 178.75 ± 3.46 HB. The outer surfaces' finishing turning, and burnishing was carried out directly on the wear test bench while partially dismantled. Finishing turning parameters prior to burnishing:

$n = 800$ rpm, $v = 100.5$ m/min, $f = 0.102$ mm/rev. For burnishing, a burnishing tool with an elastic pressure device is used, which allows the pressure of the burnishing device on the workpiece to be continuously adjusted.

The burnishing that was carried out was the so-called strengthening burnishing. Therefore, less importance was attached to obtaining optimal parameters of surface stereometry.

Analysis of the wear process of a burnished surface layer

The wear courses of burnished surfaces were analysed at a distance of 9,500 m. Macro photographs of the surface after the tests are presented on the example of a rolling ball burnishing surface (**Fig. 3a**), a disc (**Fig. 3b**), and a sliding ball burnishing surface (**Fig. 3c**). The surface appearance after friction of all specimens shows characteristics of friction wear. The cast iron used for the counter-specimens is one of the materials prone to so-called microstructural roughness (characteristic of multiphase materials

with significant grain size and large differences in hardness). During the contact, soft components of its structure, i.e., graphite and ferrite releases, were worn out first. Their loss resulted in the separation on the surface of protrusions from harder components of the cast-iron structure (perlite, phosphorus eutectic). These protrusions had outlines with sharp, irregular edges. As a result, they intensively wear the contact body by punching and extruding a grid of grooves on its surface oriented in the direction of relative motion. The grid of grooves appeared almost immediately after the start of the friction process. There was a quite pronounced increase in compaction and deepening of individual grooves in its initial stage. After a certain period (which can be regarded as the friction pair running-in phase), the height of the grooves formed stabilised. Further contact no longer led to a clear increase in roughness. Their height did not increase, but there was an expansion due to the interaction of the material of the sidewalls, indentations, and smaller protrusions. The separated material was in the form of microscopic chips carried away by the cooling liquid. On the surface of all the specimens, there appeared characteristics of friction wear, a grid of tiny grooves arranged parallel to the direction of movement.

The grafting phenomena were generally of secondary importance given the deeper micro-

cutting and grooving processes and did not leave any visible effects on the surface condition. In some places on the worn surface, traces of detached or remaining build-ups typical of adhesive wear were visible. Particularly intensive wear occurred on the surfaces worn with a sliding ball burnishing $R_k = 5$ mm (**Fig. 3c**). It can be assumed that with longer contact, the intensity of wear would increase (Stage III on the Lorenc curve), which could even lead to a seizure.

Particularly important from the point of view of the conducted studies was the group of disc burnishing surfaces, for which it was expected to obtain, during their formation, a contact-motion deformation pattern. It can be concluded that the wear of the disc burnishing surfaces is significantly lower than that of the rolling ball burnishing surfaces with identical processing parameters. A contact-motion deformation pattern was also expected for the sliding ball burnishing surfaces. Except for the ball burnishing surfaces with the smallest radius $R_k = 5$ mm, these surfaces also showed less wear than the surfaces processed by cavity methods.

The study showed a significant relationship between the intensity of wear and the surface roughness that varied depending on the friction distance. Changes in the roughness indicators as a function of the friction distance showed that after the running-in phase, it stabilised when the

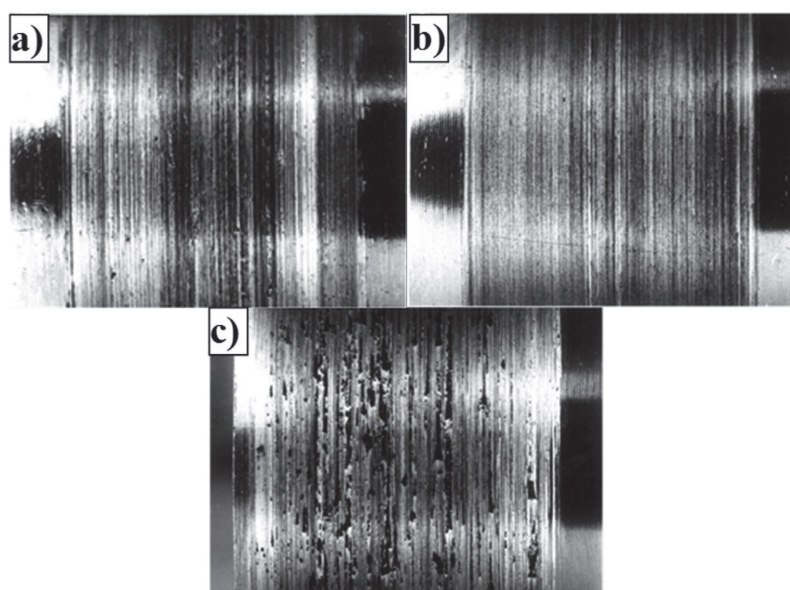


Fig. 3. Rolling burnished surfaces: a – with a ball ($F = 0.5$ kN, $R_k = 5$ mm), b – with a disc ($R_k = 10$ mm, $f = 0.255$ mm/rev., $F = 2.75$ kN), c – with a sliding ball ($F = 0.7$ kN, $R_k = 5$ mm) after friction on a distance of 9,500 m

Rys. 3. Powierzchnie nagniatane tocznie: a – kulką ($F = 0,5$ kN, $R_k = 5$ mm), b – krążkiem ($R_k = 10$ mm, $f = 0,255$ mm/obr., $F = 2,75$ kN), c – ślizgowo kulką ($F = 0,7$ kN, $R_k = 5$ mm) po tarcie na drodze 9500 m

roughness changed most significantly, and further contact did not cause such significant changes in the analysed parameters. In the course of wear on the rolling burnished surfaces, their roughness changed from technological values of $R_a = 0.2\text{--}0.8\ \mu\text{m}$ to final values of $R_a = 1\text{--}2\ \mu\text{m}$. For the sliding ball burnished wear surfaces characterised by a high technological roughness $R_a = 0.8\text{--}1.5\ \mu\text{m}$, the wear did not lead to any significant changes in roughness.

It is noticeable that not the initial roughness, which is one of the basic parameters of the technological surface layer, but the friction conditions determined the roughness formed during exploitation. For each friction pair, a change in the roughness of the contact elements occurred until the so-called equilibrium roughness was achieved, which can be defined as the roughness formed on the frictionally contact surfaces after the running-in phase. The equilibrium roughness did not depend on the initial (technological) roughness but the type and properties of the friction materials and the conditions of the friction process. It was found that it could be either smaller or larger than the initial. During the period of so-called stabilised wear following running-in, the equilibrium roughness was still recreated and remained constant throughout the period. It follows from the above considerations that any significant change in the contact conditions must be accompanied by a further run-in, as a new equilibrium state must be generated. The technological roughness determined the tribological parameters of the sliding contact mainly during the initial wear period (run-in period). It was noticeable that during wear, the nominal contact area was significantly larger than the actual contact area, and the pressures in the micro-areas of the contact zone often exceeded the permissible critical values. Due to wear, increased surface micro-roughness came into contact with each other. In the micro-areas of surface contact, the stresses exceeded the plasticising stresses, which fundamentally changed the material properties of the surface layer and, as a result, led to the deformation of the micro-areas of the roughness structure. These changes progressed deep into the material as it was being worn, i.e., as the friction process continued.

From the point of view of learning and explaining the mechanism of phenomena occurring during the process of simulated exploitation, it would be possible to observe the worn surfaces microscopically (**Fig. 4**). Digital processing of the

obtained stereometry image makes it possible to select any part of the recorded area, and it is also possible to digitally filter out a shape (e.g., cylinder) from the recorded area. The image of the analysed stereometry is then obtained and developed on the plane. A very precise "photographic" analysis of the recorded area is possible (**Fig. 5a**), as well as the analysis of any selected area of the stereometric image of the analysed surface (**Fig. 5b**) as well as the determination of SGP parameters.



Fig. 4. Stereometric image of the area of the transition zone between the non-friction and the friction area – disc burnished surface ($R_k = 10\ \text{mm}$, $f = 0.255\ \text{mm/rev.}$, $F = 2.75\ \text{kN}$) after wearing on a distance of 9,500 m

Rys. 4. Stereometryczny obraz obszaru strefy przejścia pomiędzy obszarem nie biorącym udziału w tarceniu i po tarceniu – powierzchnia nagniatana krążkiem ($R_k = 10\ \text{mm}$, $f = 0,255\ \text{mm/obr.}$, $F = 2,75\ \text{kN}$) po zużyciu na drodze 9 500 m

The test carried out produced stochastic roughness profiles in all the cases analysed, and the ordinate distribution of the profile was close to a normal distribution. Presumably, the profile obtained results from accidental grooving and micro-cutting by hard components of the cast-iron structure and products of wear sliding over the contact surface. An example, typical for the obtained measurement results, of the progress of the material share curve and the distribution of ordinates of the profile is presented in **Fig. 6**.

In the course of the study, it was found that the wear of the surface led to the obtaining of a surface roughness characteristic for a given friction pair and the conditions of contact between the friction elements. This increased the roughness of surfaces having a small initial roughness after burnishing and decreased for surfaces having the highest roughness after burnishing (especially after sliding ball burnishing). For the rolling burnishing surfaces, it is possible to distinguish those treatment parameters,

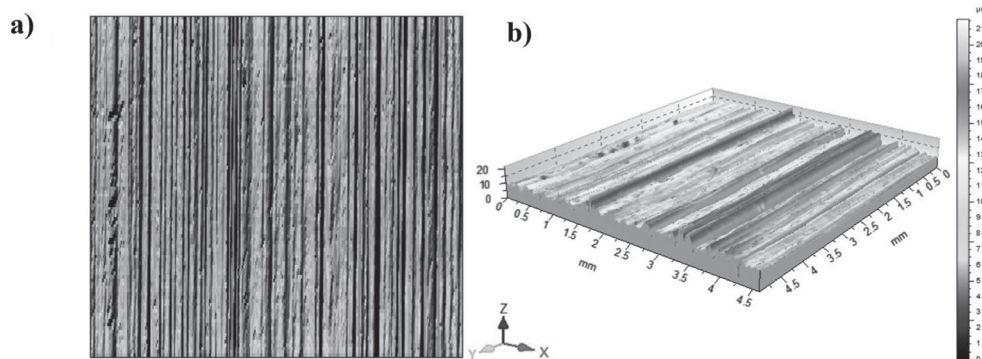


Fig. 5. Roughness of the area subjected to wear: a – "photographic" image, b – stereometric view – disc burnished surface ($R_k = 10$ mm, $f = 0.255$ mm/rev., $F = 2.75$ kN) after wear on a distance of 9 500 m

Rys. 5. Chropowatość obszaru poddanego zużyciu: a – obraz „fotograficzny”, b – widok stereometryczny – powierzchnia nagniatana krążkiem ($R_k = 10$ mm, $f = 0,255$ mm/obr., $F = 2,75$ kN) po zużyciu na drodze 9500 m

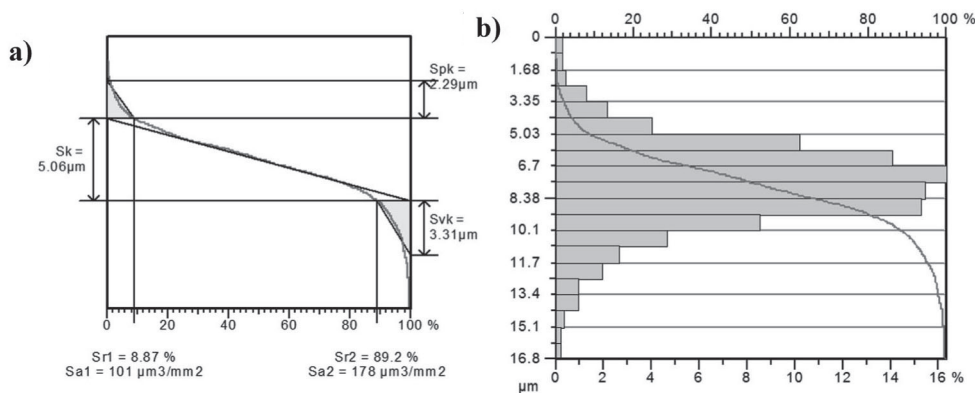


Fig. 6. Determination of the characteristic curve of the load-bearing capacity of the area – S_k method (a) and the distribution of the ordinates of area (b) – disc burnished surface ($R_k = 10$ mm, $f = 0.255$ mm/rev., $F = 2.75$ kN) after friction on a distance of 9,500 m

Rys. 6. Wyznaczenie charakterystyki krzywej nośności obszaru – metoda S_k (a) i rozkładu rzędnych obszaru (b) – powierzchnia nagniatana krążkiem ($R_k = 10$ mm, $f = 0,255$ mm/obr., $F = 2,75$ kN) po tarcii na drodze 9500 m

after which the changes in roughness and wear were the smallest. There was generally a reduction in roughness for the surface, with the highest initial roughness for sliding burnishing surfaces.

Microscopic observations of the course of the wear process were carried out on the surfaces of a rolling ball and disc burnishing after friction at 9,500 metres. Photographs were taken with a PHILIPS XL 30 scanning electron microscope.

On the ball's burnished surface after friction (Fig. 7a), one can observe a clear directionality of the structure, resulting from the applied method of burnishing and the occurring wear processes. The analyses carried out (Fig. 7b) revealed the existence of a layer of material just below the machined surface, at a depth of $0 \div 10$ μm , which differs from the material lying deeper (Beilleby layer). This

layer, containing particles absorbed by the material during the machining process, may protect the material structure against contact. Presumably, the surface layer structure features formed in this way significantly determine the progress of tribological wear. This layer had been removed by wear near the material's surface (formed during burnishing), and a new layer formed in its place, characterised by a distinctly different colour. This layer contained friction-plated particles, probably originating from the material of the cast iron counter-specimen. A clear fraying of material surface fragments, caused by friction with visible areas of shallower and deeper scratches, was also observed.

The image of the disc burnished surface after friction (Fig. 8a) was similar to that of the ball burnished surface. Wear of this surface led, as

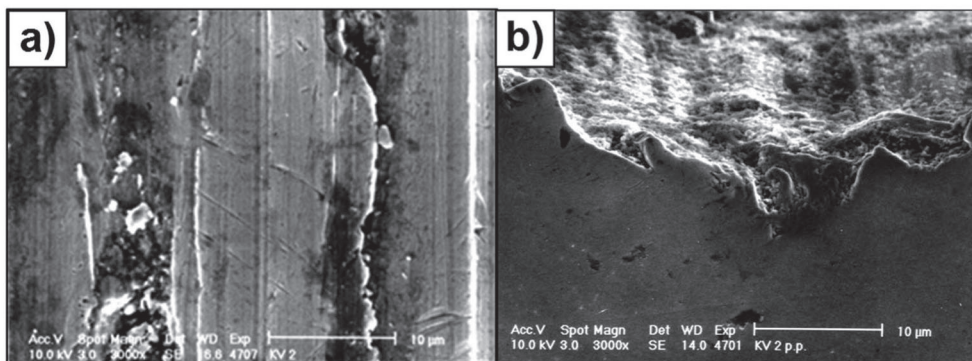


Fig. 7. Stereometric image (a) and structure of the surface layer (b) ball rolling burnishing surface $F = 5 \text{ kN}$, $R_k = 9.25 \text{ mm}$ after wearing on a distance of 9,500 m

Rys. 7. Obraz stereometrii (a) i struktura warstwy wierzchniej (b) powierzchni nagniatanej tocznie kulką $F = 5 \text{ kN}$, $R_k = 9,25 \text{ mm}$ po zużyciu na drodze 9500 m

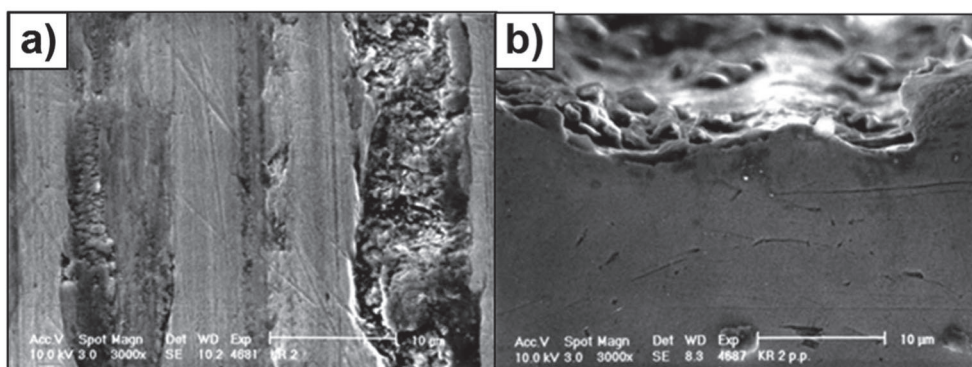


Fig. 8. Stereometric image (a) and structure of the surface layer (b) disc rolling burnishing surface $R_k = 15 \text{ mm}$, $f = 0.45 \text{ mm/rev.}$, $F = 5 \text{ kN}$ after wear on a distance of 9,500 m

Rys. 8. Obraz stereometrii (a) i struktura warstwy wierzchniej (b) powierzchni nagniatanej tocznie krążkiem $R_k = 15 \text{ mm}$, $f = 0,45 \text{ mm/obr}$, $F = 5 \text{ kN}$ po zużyciu na drodze 9500 m

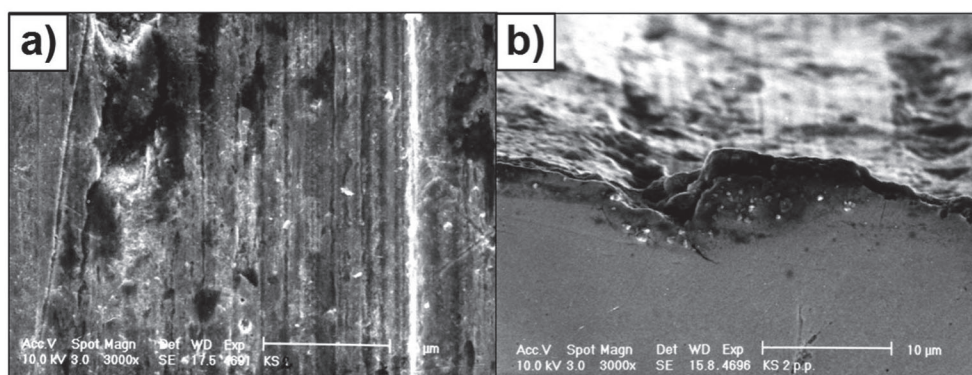


Fig. 9. Stereometric image (a) and structure of the surface layer (b) of the surface with a ball sliding burnishing $F = 1.2 \text{ kN}$, $R_k = 9.25 \text{ mm}$ after wearing on a distance of 9,500 m

Rys. 9. Obraz stereometrii (a) i struktura warstwy wierzchniej (b) powierzchni nagniatanej ślizgowo kulką $F = 1,2 \text{ kN}$, $R_k = 9,25 \text{ mm}$ po zużyciu na drodze 9500 m

in the case of the rolling ball burnished surface, to form a grid of grooves oriented following the friction direction. Traces of micro-grafting and

visible grooves and tears in the material, probably caused by the grafting process, were also observed.

The cross-section (**Fig. 8b**) revealed characteristic surface fraying caused by friction.

The process of wear on the surface of the ball sliding burnishing occurred differently than on the surfaces of the rolling burnishing. The characteristic irregular structure and fraying appeared on these surfaces already during their formation (**Fig. 9**). The resulting roughness of these surfaces was significantly higher. Within the surface layer, a characteristic layer of material appeared, strongly and repeatedly deformed by the sliding action of the tool. The friction process led to a structure covered with deep grooves and tears (**Fig. 9a**). The fusions appearing in the whole area of the friction zone on the material surface were also visible. Also, noticeable (**Fig. 9b**) was a grid of grooves oriented in the direction of friction, characteristic of frictional wear. However, the surface was much clearer than that of the rolling burnished surfaces, with deep pitting and tears due to the fusion and chipping of the material at the non-coherent points, probably caused by the over-burnishing of the surface layer.

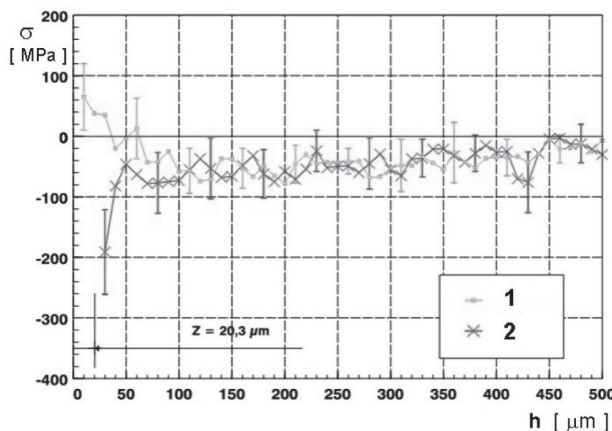


Fig. 10. Example of the distribution of circumferential stresses determined for the surface of a disc rolling burnishing before (1) and after (2) friction on a distance of 9,500 m. Burnishing parameters: force $F = 0.5$ kN, feed rate $f = 0.068$ mm/rev, radius of curvature of the disc's outline $R_k = 15$ mm

Rys. 10. Przykładowy rozkład naprężeń obwodowych wyznaczony dla nagniatanej tocznie krążkiem powierzchni przed (1) i po tarcu (2) na drodze 9500 m. Parametry obróbki nagniataniem: siła $F = 0,5$ kN, posuw $f = 0,068$ mm/obr., promień krzywizny zarysu krążka $R_k = 15$ mm

In the course of the conducted analyses, it was also possible to trace the changes that the process

of wear induced in the state of stresses occurring in the surface layer (**Fig. 10**) as a result of burnishing treatment (depending on the applied treatment parameters). The following pattern is noteworthy: the burnishing removed the remaining tensile stresses after the preceding treatment and replaced them with compressive ones. After wear, there was a clear increase in the average value of compressive stresses in the circumferential direction (concerning wear). The changes in the axial direction were in the opposite direction, i.e., they led to a reduction in the compressive stress values occurring in the surface layers after the ball and roller burnishing.

Determination of test object function

In the presented study, the input values were the burnishing parameters (tool roundness radius, burnishing force and, in the case of disc burnishing, also the burnishing feed). The proposed range of variation of individual parameters covered the typical range of parameters used in the burnishing technology of the analysed surfaces. The ranges of variation of the input values were selected based on the general rules for the selection of burnishing parameters in such a way that any combination of them was feasible and reasonable from the point of view of the study. The output quantity analysed was the wear.

The influence of two input values of ball burnishing (ball radius $R_k - 5 \div 13.5$ mm and burnishing tool pressure $F - 0.5 \div 5$ kN) on the course and effects of wear were analysed in the test. The remaining burnishing parameters were constant and amounted to $v = 10$ m/min and $f = 0.102$ mm/rev. A static determined, complete experimental plan (PS/DK - 3^2) with $n_k = \text{const.} = 3$ was adopted for the thus assumed test area. With a relatively small number of systems $n = 9$, this plan ensures maximum informativeness and high efficiency of the conducted tests.

The second group of tests consisted of disc burnishing surfaces. In the case of disc burnishing, three treatment parameters were taken as variables - three input values (disc radius of curvature R_k , tool clamping force F , and feed f). The remaining burnishing parameters were constant throughout the tests and were $v = 10$ m/min and the diameter of the burnishing disc $d = 39$ mm. A static determined poli-selective Hartley Special Experiment Plan (PS/DS - $P:Ha_3$) based on a hypercube (hS). The choice of the plan was based on its particularly good efficiency combined with fairly good

informativeness. The choice of the hypercube-based plan (hS) rather than the more informative hypersphere-based plan (hK) was based on the desire to minimise the number of input values.

The third group of the tested specimens consisted of sliding ball burnishing surfaces. For these surfaces, the effect of two input values (ball radius $R_k - 5 \div 13.5$ mm and burnishing tool pressure $F - 0.2 \div 1.2$ kN) on the course and effects of wear were tested. The remaining parameters of burnishing were constant and amounted $v = 10$ m/min and $f = 0.102$ mm/rev. A static determined complete experimental plan (PS/DK - 3^2) with $n_k = \text{const.} = 3$ was assumed.

Using digital processing of the obtained measurement results, they were approximated by the function of the tested object. For the assumed two-dimensional area of the ball burnishing surfaces, the measurement results were approximated by functions $f(x,y)$ – algebraic polynomials (linear, quadratic and interaction components). In this way, the test object function was obtained, i.e., the dependence of the tested surface layer parameters

on the input values (burnishing force F and ball radius R_k). A similar procedure was adopted for the assumed three-dimensional area of testing surfaces burnished with a disc. The test object functions $f(x, y, z)$ were obtained, i.e., the dependence of the tested surface layer parameters on the input values (radius of disc curvature R_k , burnishing force F , and feed rate f). The choice of the form of the approximating function was conditioned by its relatively simple form, ensuring ease of calculations. The functions determined for the surfaces to be burnished with a disc $f(x, y, z)$ are four-dimensional functions, and as such, they cannot be represented graphically. Only a graphical representation, which is a cross-section of a given function at a constant value of the radius of curvature, feed or force, is possible.

The results of the performed tests after statistical analysis allowed for describing the tested dependencies of wear (Z) on the burnishing parameters (tool radius of curvature R_k , burnishing force F , and in case of disc burnishing, also burnishing feed f) with the following polynomials:

for a rolling ball burnishing surface (**Fig. 11a**):

$$Z = 26.42 + 10.18F - 4.64R_k - 0.35F^2 - 0.86F \cdot R_k + 0.39R_k^2$$

for a sliding ball burnishing surface (**Fig. 11b**):

$$Z = 188.03 - 88.95F - 26.20R_k + 36.68F^2 + 2.61F \cdot R_k + 1.10R_k^2$$

for a disc burnishing surface (**Fig. 12**):

$$Z = 58.63 - 3.98R_k - 124.46f - 7.60F + 0.15R_k^2 + 0.26R_k \cdot f + 132.19f^2 + 19.27f \cdot F + 0.43F^2$$

Graphical interpretations of the results are shown in **Figures 11** and **12**. These polynomials allow for optimisation of the burnishing process. The analysis of the obtained polynomials allows us to state that the optimum processing parameters for all groups of surfaces can be determined (in the considered range of parameter variation), ensuring minimum wear. And so for rolling ball burnishing surfaces – $Z_{\min} = 14.8$ μm for $F = 0.5$ kN i $R_k = 6.54$ mm; of surfaces to be disc rolling burnished – $Z_{\min} = 5.4$ μm for $R_k = 12.75$ mm, $f = 0.42$ mm/rev. and $F = 0.5$ kN and $Z_{\min} = 5.7$ μm for $R_k = 12.65$ mm, $f = 0.093$ mm/rev. and $F = 5$ kN; of surfaces to be sliding burnished $Z_{\min} = 8.4$ μm for $F = 0.825$ kN and $R_k = 10.87$ mm. The value of the ball rolling burnishing force (**Fig. 11a**) must be selected according to the tool radius to ensure the correct unit pressure. Too high or too low a force leads to increased wear. Increasing the feed rate during disc

burnishing (**Fig. 12**) leads to a significant decrease in the wear value, but only for low burnishing forces. At higher forces, an increase in the feed rate probably causes excessive contact stresses in the contact area during the burnishing process and, as a result, leads to material over-compression. This is also confirmed by analysing the influence of the radius of curvature of the tool on the value of the wear obtained. In almost the entire range of disc curvatures ($R_k < 5; 13.5$), regardless of the force and feed value, an increase in the radius of curvature led to a decrease in the wear value. In the case of ball sliding burnishing surfaces (**Fig. 11b**), an unfavourable influence of using a tool with too small curvature can also be observed. In all cases, the results of the performed analysis allow for an estimated selection of optimum processing parameters that ensure minimum wear value for a given shape and profile of the tool.

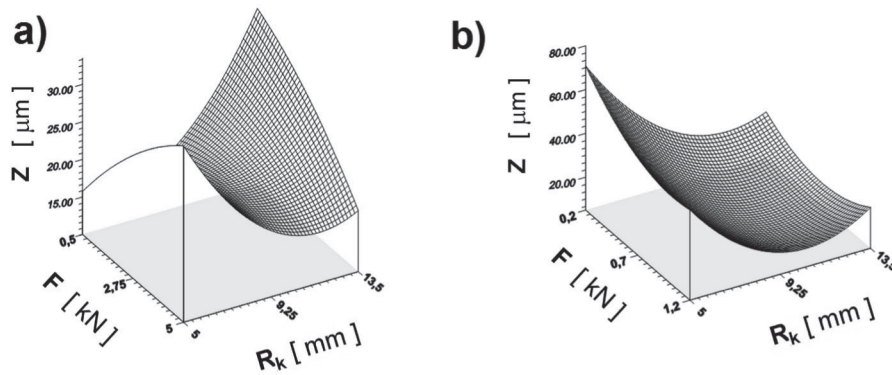


Fig. 11. Graphical representation of the dependence of the effect of burnishing parameters on wear resistance: a – ball rolling burnishing surfaces, b – ball sliding burnishing surfaces

Rys. 11. Graficzne zobrazowanie zależności wpływu parametrów obróbki nagniataniem na odporność na zużycie: a – powierzchnie nagniatane tocznie kulką, b – powierzchnie nagniatane ślizgowo kulką

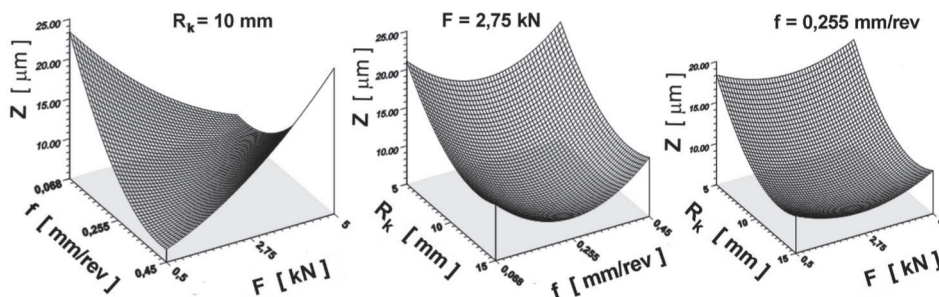


Fig. 12. Graphical representation of the dependence of the effect of the burnishing processing parameters on the wear resistance of a disc burnishing surface at a constant value of one of the treatment parameters

Rys. 12. Graficzne zobrazowanie zależności wpływu parametrów obróbki nagniataniem na odporność na zużycie powierzchni nagniatanej krążkiem przy stałej wartości jednego z parametrów obróbki

Long-term wear process tests

In order to confirm the beneficial effect of the change in a deformation pattern characteristic of disc burnishing, the long-term wear tests were carried out over a distance of 47,500 m. The test specimens were pressure burnished with a ball and disc rolling and ball sliding. A contact time of 20 h was established. This allowed the wear of a layer with a thickness exceeding the depth of the material layer with the greatest degree of strengthening induced by the burnishing treatment ($Z = 0.05 \div 0.15$ mm). The technological parameters of treatment of these surfaces were selected in the central points of the testing areas described previously. The results of wear testing and changes in the friction coefficient are presented in Fig. 13.

Analysis of the changes in the wear values of the specimens over a friction distance of 47,500

m shows a significant predominance of the disc burnished surfaces and the ball sliding burnished surfaces (for which a contact-motion deformation pattern was expected) over the ball rolling burnished surfaces (for which a contact-motion deformation pattern was predicted). After a friction distance of 10,000 m, the wear values of all surfaces were similar, and further contact revealed distinct differences in the behaviour of individual groups of surfaces. For these parameters, the final wear (along with the friction distance of 47,500 m) of ball burnishing surfaces was more than twice as high as that of the ball sliding burnishing surfaces of the same profile (with smaller forces applied) and more than three times as high as that of disc burnishing surfaces of the same radius of curvature and with identical technological parameters of treatment (force, feed, burnishing speed). The

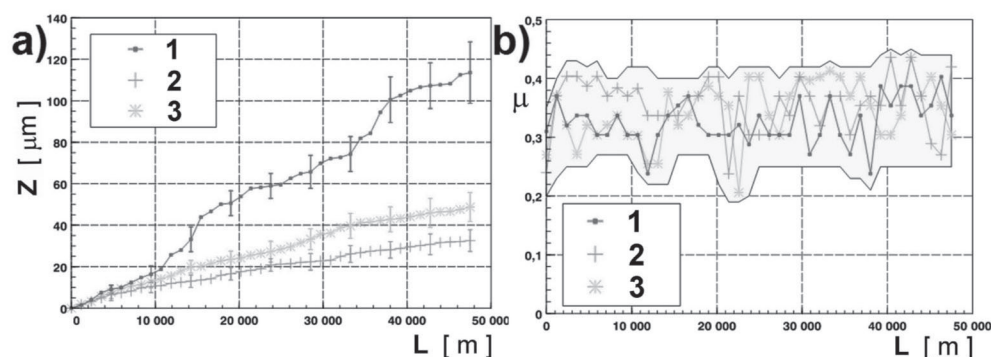


Fig. 13. Dependence of wear (a) and friction coefficient (b) on the friction distance for the surface burnished/cast iron combination: 1 – ball rolling burnishing ($F = 2.75$ kN, $R_k = 9.5$ mm), 2 – disc rolling burnishing ($F = 2.75$ kN, $f = 0.255$ mm/rev., $R_k = 10$ mm), 3 – ball sliding burnishing ($F = 0.7$ kN, $R_k = 9.5$ mm)

Rys. 13. Zależność zużycia (a) i współczynnika tarcia (b) od drogi tarcia w skojarzeniu nagniatane powierzchnie/żeliwo: 1 – nagniatanie toczne kulką ($F = 2,75$ kN, $R_k = 9,5$ mm), 2 – nagniatanie toczne krążkiem ($F = 2,75$ kN, $f = 0,255$ mm/obr., $R_k = 10$ mm), 3 – nagniatanie ślizgowo kulką ($F = 0,7$ kN, $R_k = 9,5$ mm)

probable reason for these differences seems to be a change in the nature of the processes occurring in the deformation zone, resulting from the kinematics of the burnishing treatment. During the treatment of disc and ball sliding burnishing surfaces, there were additional forces tangential to the surface of the workpiece to form a deformation zone. It was also observed that during friction, after an initial increase, the coefficient of friction stabilised during the run-in period and slightly decreased. Subsequent contact, especially of the sliding burnishing and ball rolling burnishing surfaces, was characterised by significant fluctuations of the friction coefficient value. Certain instabilities can explain this in the course of wear of friction surfaces caused by their considerable roughness, leading to deformations and destruction of micro-pitting and formation and removal of grafting. After certain stages of instability, the friction surfaces presumably reached the roughness characteristic of a given friction pair again, and wear stabilised. The surface subjected to disc burnishing up to the end of the wear period was in the stable wear period (period II of the Lorenc curve), whereas the surfaces subjected to the ball rolling and sliding burnishing, and particularly the surface subjected to the ball rolling burnishing, in the last phase of friction was probably approaching the unstable wear period, i.e., the so-called emergency wear period. This could be additionally evidenced by clearly visible fluctuations of the friction coefficient value.

SUMMARY

The tests confirmed that disc burnishing surfaces (for which it was intended to obtain a more favourable contact-motion deformation pattern due to the appearance of additional forces tangential to the surface of the material in the process of forming the deformation zone during burnishing) wore under the same friction conditions and under similar treatment conditions (the same contact forces and similar radii of curvature of burnishing tools) significantly less than ball burnishing surfaces (for which a contact-motion deformation pattern was obtained). In both groups of specimens, it was noticeable that there was such a value of unit pressure (depending on the ball radius or the radius of curvature of the disc and the burnishing force), for which the wear was the lowest. A group of sliding burnishing surfaces was also tested. Despite the application of a contact-motion deformation pattern, the results obtained were not as promising as for the rolling burnishing surfaces. It was probably caused by obtaining a very unfavourable stereometric structure for this group of surfaces, causing significant wear values (especially in the run-in period).

The results of the presented tests allow for a deliberate control of the functional features of the surface layers formed by burnishing by changing the treatment method and the values of the technological parameters used in the process. This is facilitated by the determined functions of the test object (surface layer being burnished) relating the technological parameters of treatment

to the value of wear. For all groups of the analysed burnished surfaces, it has become possible to determine the optimum treatment parameters that ensure minimum wear: for ball rolling burnishing surfaces $Z_{\min} = 14.8 \mu\text{m}$ for $F = 0.5 \text{ kN}$ and $R_k = 6.54 \text{ mm}$, disc rolling burnishing $Z_{\min} = 5.7 \mu\text{m}$ for $R_k = 12.75 \text{ mm}$, $f = 0.42 \text{ mm/rev.}$ and

$F = 0.5 \text{ kN}$ and ball sliding burnishing $Z_{\min} = 8.4 \mu\text{m}$ for $F = 0.825 \text{ kN}$ and $R_k = 10.87 \text{ mm}$. The optimum parameters were determined within the considered ranges of variation of technological treatment parameters. These ranges were selected to cover the typical scope of technological parameters used in the analysed burnishing process.

REFERENCES

1. Przybylski W.: *Technologia obróbki nagniataniem*, WNT, Warszawa 1987.
2. Przybylski W.: *Low plasticity burnishing processes. Fundamentals, tools and machine tools*. Institute for sustainable technologies. National research institute in Radom, Radom 2019.
3. Ballanda P., Tabourot L., Degrea F., Moreaub V.: *Mechanics of the burnishing process*. *Precision Engineering* 37 (2013), pp. 129–134.
4. Korzyński M.: *Nagniatanie ślizgowe*, WNT, Warszawa 2007.
5. Tubielewicz K.: *Analiza zjawisk towarzyszących odkształceniu warstwy wierzchniej w procesie nagniatania*, Wydawnictwo Politechniki Częstochowskiej. Series Monographs No 13, Częstochowa 1990.
6. Tubielewicz K.: *Analiza naprężeń powstających w warstwie wierzchniej podczas procesu nagniatania*, Wydawnictwo Politechniki Częstochowskiej, Częstochowa 1993.
7. El-Tayeb N.S.M., Low K.O., Brevern P.V.: *Enhancement of surface quality and tribological properties using ball burnishing process*. *Machining Science and Technology*, 12 (2008), pp. 234–248 Taylor & Francis Group, LLC.
8. El-Tayeb N.S.M., Low K.O., Brevern P.V.: *Influence of roller burnishing contact width and burnishing orientation on surface quality and tribological behaviour of Aluminium 6061*, *Journal of Materials Processing Technology* 186 (2007), pp. 272–278.
9. El-Tayeb N.S.M., Low K.O., Brevern P.V.: *On the surface and tribological characteristics of burnished cylindrical Al-6061*, *Tribology International* 42 (2009), pp. 320–326.
10. Korzyński M.: *Modeling and experimental validation of the force-surface roughness relation for smoothing burnishing with a spherical tool*, *International Journal of Machine Tools & Manufacture* 47 (2007), pp. 1956–1964.
11. Korzyński M., Lubas J., Świrad S., Dudek K.: *Surface layer characteristics due to slide diamond burnishing with a cylindrical-ended tool*, *Journal of Materials Processing Technology* 211 (2011), pp. 84–94.
12. Lin Y.C., Wang S.W., Lai H.Y.: *The relationship between surface roughness and burnishing factor in the burnishing process*, *Int J Adv Manuf Technol* (2004), 23, pp. 666–671.
13. Grzesik W., Żak K.: *Modification of surface finish produced by hard turning using superfinishing and burnishing operations*, *Journal of Materials Processing Technology* 212 (2012), pp. 315–322.
14. Frihat M.H., Al Quran F.M.F., Al-Odat M.Q.: *Experimental investigation of the influence of burnishing parameters on surface roughness and hardness of brass alloy*, *J Material Sci Eng* 5 (2015), p. 216.
15. Hassan A.M., Al-Bsharat A. S.: *Influence of burnishing process on surface roughness, hardness, and microstructure of some non-ferrous metals*, *Wear* 199 (1996), pp. 1–8.
16. Sagbas A.: *Analysis and optimization of surface roughness in the ball burnishing process using response surface methodology and desirability function*. *Advances in Engineering Software* 42 (2011), pp. 992–998.

17. Chodór J., Kukielka L.: Komputerowe modelowanie i symulacja procesu przemieszczania ostrza po sprężystolepko-plastycznym podłożu na przykładzie nagniatania ślizgowego. Praca zbiorowa pod redakcją Włodzimierza Przybylskiego „Współczesne problemy w technologii obróbki przez nagniatanie”. Wydawnictwo Politechniki Gdańskiej, Gdańsk 2008. Vol. 2, pp. 39–46.
18. Kułakowska A., Kukielka L.: Analiza numeryczna wpływu odchyłek zarysu nierówności powierzchni po toczeniu na wybrane właściwości warstwy wierzchniej wyrobu nagniatanego. Praca zbiorowa pod redakcją Włodzimierza Przybylskiego „Współczesne problemy w technologii obróbki przez nagniatanie”. Wydawnictwo Politechniki Gdańskiej, Gdańsk 2008. Vol. 2, pp. 127–134.
19. Malleswara Rao J.N., Chenna Kesava Reddy A., Rama Rao P.V.: The effect of roller burnishing on surface hardness and surface roughness on mild steel specimens International Journal of Applied Engineering Research, Vol. 1, No 4, (2011), pp. 777–785.
20. Zaleski K., Skoczylas A.: Effect of slide burnishing on the surface layer and fatigue life of titanium alloy parts Advances in materials science, Vol. 19, No. 4 (62), December 2019.
21. Zaborski A., Tubielewicz K.: Analiza przebiegu procesu zużywania warstwy wierzchniej po nagniataniu. Praca zbiorowa pod redakcją Włodzimierza Przybylskiego „Współczesne problemy w technologii obróbki przez nagniatanie”. Wydawnictwo Politechniki Gdańskiej, Gdańsk 2005. Chapter III. 12, pp. 255–264.
22. Tubielewicz K., Zaborski A.: Przebieg procesu zużywania nagniatanych warstw wierzchnich. Tribologia 4/2008, pp. 165–174.
23. Saini D., Kapoor M., Jawalkar CS.: Parametric analysis of mild steel specimens using roller burnishing process. International Refereed Journal of Engineering and Science, Vol. 6, Issue 3 (March 2017), pp. 45–51.
24. Zaborski A.: Analiza formowania strefy deformacji w procesie nagniatania. Wydawnictwo Politechniki Częstochowskiej. Series Monographs no 260, Częstochowa 2013.
25. Zaborski A.: Komputerowo wspomagane pomiary parametrów geometrycznych strefy deformacji w procesie nagniatania, Mechanik 8–9/2019, pp. 548–550.